THE JOURNAL OF BIOLOGICAL CHEMISTRY VOL. 283, NO. 36, pp. 24899–24908, September 5, 2008
Printed in the U.S.A.

Regulation of Nuclear Import/Export of Carbohydrate Response Element-binding Protein (ChREBP)

*INTERACTION OF AN α-HELIX OF ChREBP WITH THE 14-3-3 PROTEINS AND REGULATION BY PHOSPHORYLATION**

Received for publication, June 4, 2008, and in revised form, July 2, 2008 Published, JBC Papers in Press, July 7, 2008, DOI 10.1074/jbc.M804308200

Haruhiko Sakiyama[‡], R. Max Wynn[‡], Wan-Ru Lee[‡], Masashi Fukasawa[‡], Hiroyuki Mizuguchi[§], Kevin H. Gardner[‡¶], Joyce J. Repa[‖], and Kosaku Uyeda[‡1]**

*From the Departments of [‡]Biochemistry, [¶]Pharmacology and [‖]Physiology, University of Texas Southwestern Medical Center, Dallas, Texas 75390, the [§]Department of Pharmaceutical Sciences, Tokushima University, Tokushima, Japan, and the **Dallas Veterans Affairs Medical Center, Dallas, Texas 75216*

Carbohydrate response element-binding protein (ChREBP) is a glucose-responsive transcription factor that plays a critical role in the glucose-mediated induction of gene products involved in hepatic glycolysis and lipogenesis. Glucose affects the activity of ChREBP largely through post-translational mechanisms involving phosphorylation-dependent cellular localization. In this work we show that the N-terminal region of ChREBP (residues 1–251) regulates its subcellular localization via an interaction with 14-3-3. 14-3-3 binds an α-helix in this region (residues 125–135) to retain ChREBP in the cytosol, and binding of 14-3-3 is facilitated by phosphorylation of nearby Ser-140 and Ser-196. Phosphorylation of ChREBP at these sites was essential for its interaction with CRM1 for export to the cytosol, whereas nuclear import of ChREBP requires dephosphorylated ChREBP to interact with importin α. Notably, 14-3-3 appears to compete with importin α for ChREBP binding. 14-3-3β bound to a synthetic peptide spanning residues 125–144 and bearing a phosphate at Ser-140 with a dissociation constant of 1.1 μM, as determined by isothermal calorimetry. The interaction caused a shift in the fluorescence maximum of the tryptophan residues of the peptide. The corresponding unphosphorylated peptide failed to bind 14-3-3β. These results suggest that interactions with importin α and 14-3-3 regulate movement of ChREBP into and out of the nucleus, respectively, and that these interactions are regulated by the ChREBP phosphorylation status.

The liver is the principal organ responsible for the conversion of excess dietary carbohydrates to stored triglyceride. Metabolism of carbohydrates in the liver provides a substrate, acetyl-CoA, for triglyceride synthesis and induces expression of liver pyruvate kinase (LPK)[2] and lipogenic enzymes independently of insulin. The mechanism by which excess carbohydrates induce expression of lipogenic enzyme genes became clearer with the discovery of carbohydrate response element-binding protein (ChREBP) (1). When glucose availability is low, a phosphorylated, inactive pool of ChREBP is mainly localized in the cytosol. As the glucose level rises, the concentration of the pentose phosphate shunt intermediate xylulose 5-phosphate (Xu5P) increases, activating a specific protein phosphatase, PP2A-ABδC, which leads to dephosphorylation of ChREBP (2). The dephosphorylated ChREBP translocates to the nucleus where it binds to carbohydrate response elements within the promoters of LPK and genes involved in hepatic lipogenesis to couple glucose utilization and fatty acid synthesis (3, 4).

ChREBP is a large transcription factor of 96 kDa containing several functional domains, including nuclear export (NES) and nuclear import signals (NLS), a DNA binding bHLH/ZIP domain, and proline-rich regions (Fig. 1*A*). Increased glucose levels after meals lead to the conversion of inactive ChREBP (phosphorylated) in the cytosol to an activated/dephosphorylated state via Xu5P-activated PP2A. This dephosphorylated ChREBP then translocates to the nucleus to initiate transcription. This model of ChREBP regulation by subcellular localization controlled by a phosphorylation/dephosphorylation mechanism is based on the observations that hepatocytes incubated with protein kinase inhibitors exhibit an increase in both nuclear localization and DNA binding efficiency of ChREBP, whereas treatment with protein phosphatase inhibitors blocks nuclear import (4). Moreover, a mutated ChREBP (S196D-ChREBP) that mimics the phospho-ChREBP produced by protein kinase A (PKA) localizes to the cytosol, whereas a mimic of the dephosphorylated form (S196A-ChREBP) migrates into the nucleus in cultured hepatocytes. Once inside the nucleus, other phosphorylated residues of ChREBP (Ser-626 and Thr-666) are dephosphorylated by nuclear Xu5P-activated PP2A, thus enhancing ChREBP DNA binding and transactivation (4, 5).

Based on these observations, we previously proposed that subcellular localization of ChREBP is regulated by the phosphorylation state of Ser-196, and the transcriptional activation activity of ChREBP is regulated by the phosphorylation states of

* The costs of publication of this article were defrayed in part by the payment of page charges. This article must therefore be hereby marked "*advertisement*" in accordance with 18 U.S.C. Section 1734 solely to indicate this fact.

[1] To whom correspondence should be addressed. E-mail: Kosaku.Uyeda@utsouthwestern.edu.

[2] The abbreviations used are: LPK, liver pyruvate kinase; ChREBP, carbohydrate response element-binding protein; ChREBP-C, residues 252–865 of ChREBP; ChREBP-N, residues 1–251 of ChREBP; ITC, isothermal titration calorimetry; NES, nuclear export signal; NLS, nuclear localization signal; PKA, protein kinase A or cAMP-dependent protein kinase; Xu5P, xylulose 5-phosphate; TBS, Tris-buffered saline; GST, glutathione *S*-transferase; DMEM, Dulbecco's modified Eagle's medium; HA, hemagglutinin; GFP, green fluorescent protein; WT, wild type.

Ser-626 and Thr-666 (4). This mechanism of high-glucose activation of ChREBP by dephosphorylation and inactivation by PKA-dependent phosphorylation is entirely consistent with regulation of carbohydrate metabolism and lipogenesis pathways in the liver by the opposing effects of glucose on one hand and glucagon and cyclic AMP (cAMP) on the other.

Recently this phosphorylation-mediated regulatory pathway for ChREBP has received further scrutiny (6) based on the findings that hepatocyte cAMP levels do not change with alterations in glucose concentration, and that certain mutated forms of ChREBP retain the ability to respond to high glucose. These results suggest that regulation of ChREBP may involve additional mechanisms beyond control of the phosphorylation status of the described PKA-targeted sites.

Li *et al.* (7) proposed an alternate mechanism of glucose-mediated regulation of ChREBP after they identified a glucose-sensing module in the N-terminal region of ChREBP (residues 1–400). Under low-glucose conditions, an inhibitory domain keeps ChREBP in an inactive state until it is somehow relieved upon exposure to high glucose. According to this model, activation in response to glucose is mediated by an intramolecular mechanism rather than phosphorylation. Although this mechanism may explain activation of ChREBP under low glucose conditions, it fails to explain the additional activation in high glucose (11).

Using a yeast two-hybrid strategy, Merla *et al.* (8) found that endogenous 14-3-3 proteins can interact with ChREBP. They found that Mlx, a protein with which ChREBP must interact to bind DNA (9–12), and 14-3-3 isoforms (β, γ, ζ, and θ) all associate with the N-terminal (residues 1–297) and C-terminal (residues 584–864) portions of ChREBP. 14-3-3 proteins are known to bind to phosphorylated substrates; consistent with this, alkaline phosphatase treatment led to the complete loss of ChREBP/14-3-3 interactions. Although this finding suggested an important role for ChREBP phosphorylation in this interaction, 14-3-3 was able to bind to five mutated forms of ChREBP in which sites of phosphorylation were singly changed to alanine (S140A, S196A, S568A, S626A, and T666A) (4). Interestingly, a deletion mutant lacking residues 117–133 of ChREBP was unable to bind 14-3-3. Based on these results, it was suggested that either the interaction of 14-3-3 and ChREBP may require one or more additional factors, or that phosphorylation has an indirect effect on protein folding.

In this report we have further examined the mechanism by which glucose regulates subcellular localization of ChREBP, and the role of phosphorylation of residues Ser-140 and Ser-196 in this mechanism. Our results provide direct evidence that interaction of phosphorylated ChREBP with 14-3-3 affects movement of ChREBP between the nucleus and cytoplasm. We identified α-helical domains within the N-terminal region of ChREBP and nearby phosphorylation sites required for the interaction with 14-3-3, and demonstrated that these interactions play essential roles in regulating ChREBP localization and hence activity.

EXPERIMENTAL PROCEDURES

Chemicals and Vectors—All chemicals were purchased from Sigma unless otherwise indicated. Bacterial expression vectors for GST-importin α, GST-importin β, and mouse 14-3-3β were gifts from Dr. Y. Yoneda (Osaka University, Osaka, Japan). Expression vectors for the other human 14-3-3 proteins were gifts from Dr. Steve L. McKnight (University of Texas Southwestern Medical Center, Dallas, TX). The expression vector for RanQ69L was a gift from Dr. Yuh Min Chook (University of Texas Southwestern Medical Center). Mammalian expression vectors for CRM1 and Mlx were prepared by reverse transcriptase-PCR cloning these gene products, verifying the integrity of the cDNA products by sequencing, and subcloning these genes into the pcDNA 3.1 expression plasmid (Invitrogen).

Proteins and Peptides—GST-tagged importin α and importin β, and His-tagged mouse 14-3-3β, human 14-3-3β, human 14-3-3γ, and human 14-3-3ζ were introduced into *Escherichia coli* strain BL21. Expression of the proteins was induced by addition of isopropyl 1-thio-β-D-galactopyranoside (0.1 mM) followed by incubation at 20 °C with shaking at 120 rpm for 16 h. GST fusion proteins were purified using glutathione-Sepharose (GE Healthcare) according to the manufacturer's instructions. His-tagged proteins were purified by affinity chromatography using nickel-nitrilotriacetic acid (GE Healthcare). The peptide containing the α_2 helix of ChREBP phosphorylated at Ser-140, designated as "α_2-S140(p)," was synthesized by the Peptide Synthesis Group at the University of Texas Southwestern. The binding of this peptide to 14-3-3 was studied using isothermal titration calorimetry (ITC). A synthetic 14-3-3 target peptide (ARApSAPA) (13) was prepared by the same group and used as a positive control for protein interaction. Secondary structure analyses were performed using the JPRED prediction service (14), complemented by estimations of peptide helical propensity using the AGADIR algorithm (15).

Animals—The Veterans Affairs Medical Center Institutional Animal Care and Use Research Advisory Committee approved all animal studies. Male mice 6–10 weeks of age were housed in temperature-controlled facilities with 12-h light/dark cycles and maintained on standard rodent chow (Harlan-Teklad Mouse/Rat Diet 7002; Harlan-Teklad Premier Laboratory Diets). The high carbohydrate and high fat diets were as described before (16). The high starch diet was fed to wild type mice and ChREBP gene-deficient mice because the latter animals cannot tolerate a sucrose-containing diet (16).

Preparation of Nuclear Extracts—For determination of the subcellular distribution of ChREBP, 14-3-3, and Mlx, mice were sacrificed 2–3 h after lights came on and livers were removed immediately. Liver nuclei were isolated by differential centrifugation of liver extracts prepared according to Hattori *et al.* (17) with minor modifications. Rats were fasted for 24–48 h and then refed either the standard lab chow, the high-sucrose diet, or the high-fat diet for 48 h before tissue harvest.

Construction of Plasmids—The expression vector for His-tagged ChREBP was described previously (1), whereas GFP-tagged ChREBP was generated as follows. The coding region of ChREBP was PCR-amplified using oligonucleotides, 5′-TACCGGACTCAGATCTCGAGCGCGGGAATTCGATTATGG-3′ (forward) and 5′-TAGAATTCCCCGCGGTAGAGGTCAAGGTGGGTGGACTGG-3′ (reverse). The PCR product was digested with XhoI and SacII, then ligated into pEGFP-C3 (Clontech). FLAG-tagged ChREBP was constructed

using pExchange5A (Stratagene). Site-specific mutations were performed using the QuikChange site-directed mutagenesis kit (Stratagene) according to the manufacturer's instructions. The oligonucleotides used for site-directed mutagenesis were described previously (4).

Primary Hepatocyte Culture and Transfection with Luciferase Reporter—Isolation of primary hepatocytes from rat liver and transfection of the cells with a luciferase reporter were performed as described previously (1). Briefly, 5 h after isolation, the culture medium was replaced with DMEM without fetal bovine serum or antibiotics. Attached cells (0.5×10^5) were transfected by adding 0.2 μg of the pRL-TK reporter plasmid (containing *Renilla* luciferase as an internal control), 2.0 μg of pGL3-LPK plasmid (firefly luciferase, an experimental reporter), and 1.0 μg of His-ChREBP expression plasmid using Lipofectamine 2000 (Invitrogen) diluted with Opti-MEM (Invitrogen). Four hours later, the medium was replaced with DMEM containing 5.5 mM glucose supplemented with 1 nM insulin, 100 nM dexamethasone, 100 units/ml penicillin, 100 μg/ml streptomycin, 10% dialyzed fetal bovine serum, and either 5.5 or 27.5 mM glucose. Cells were incubated for an additional 20 h, and the luciferase reporter activity was determined using the Dual-Luciferase Reporter Assay System (Promega) according to the manufacturer's instructions.

Subcellular Localization of ChREBP—To determine the subcellular localization of ChREBP, hepatocytes were plated onto 35-mm glass-bottomed dishes (MatTek) coated with type I collagen at a density of 5.0×10^5 cells per dish, and 3.2 μg of expression plasmid encoding wild type or mutated versions of GFP-ChREBP were transfected into the attached hepatocytes by Lipofectamine 2000 as described above. For high-glucose conditions, D-glucose was added 16 h after transfection to a final concentration of 27.5 mM, and the cells were incubated for an additional 24 h. The cells were washed once with phosphate-buffered saline, and fixed with phosphate-buffered saline-buffered 4% formaldehyde for 15 min at room temperature followed by replacement with phosphate-buffered saline containing 50 mM glycine. The subcellular localization of GFP-ChREBP was determined using a confocal laser microscope. Typically three sets of about 100 fluorescent cells were counted and scored for subcellular localization, in each of three independent experiments.

Protein-Protein Interaction of ChREBP with the Import Complex—In vitro binding assays for the interaction between ChREBP, Mlx, and importins were carried out as follows. FLAG-tagged ChREBP was expressed in HEK293T cells and purified from cell lysate by incubating with beads bearing anti-FLAG antibodies in a buffer containing 10 mM Tris-HCl, pH 7.4, 150 mM NaCl, 0.5 mM EDTA, 10 mM sodium fluoride, 1% Nonidet P-40 for 1 h at 4 °C with gentle rocking.

To prepare a ChREBP-Mlx heterodimer, HA-tagged Mlx was expressed in HEK293T cells. Cell lysate containing HA-Mlx was incubated with gentle rocking for 1.5 h at 4 °C with FLAG-ChREBP-bound beads in 500 μl of reaction buffer (20 mM HEPES-KOH, pH 7.3, 110 mM potassium acetate, 2 mM magnesium acetate, 5 mM sodium acetate, 0.5 mM EGTA, and 0.01% Nonidet P-40) (18) supplemented with 0.5% bovine serum albumin and 1 tablet of Complete Mini (Roche) per 10 ml. To confirm heterodimer formation, ChREBP-bound beads with Mlx bound were eluted with SDS-PAGE sample buffer and subjected to PAGE followed by immunoblotting.

The interactions of ChREBP or ChREBP-Mlx with importin α and importin β for the nuclear import process were assayed as follows. Beads bound with ChREBP or ChREBP-Mlx were incubated with 2 μg each of homogeneous preparations of bacterially expressed GST-tagged importin α or importin β in 500 μl of transport buffer in the above reaction mixture for 1.5 h at 4 °C with gentle rocking. The beads were washed 3 times with reaction buffer (defined above) without bovine serum albumin, eluted with SDS-PAGE sample buffer, and then subjected to PAGE and immunoblotting with antibodies for importin α or β. Under these conditions, we found that Mlx had little effect on the ChREBP-importin interaction.

The interaction of ChREBP-14-3-3 complex with proteins of the nuclear export process was carried out as follows. The ChREBP-bound beads were incubated in 500 μl of reaction buffer containing 2 μg of CRM1, 5 μg of RanQ69L (which lacks GTPase activity), 2 μg of 14-3-3 (19), and 10 μM GTP for 1.5 h at 4 °C with gentle rocking. After washing the beads 3 times with reaction buffer without bovine serum albumin, proteins were eluted with SDS-PAGE sample buffer, and subjected to PAGE and immunoblotting for CRM1, 14-3-3, and ChREBP.

For PAGE and immunoblotting, protein samples were size-fractionated on an 8 or 10% SDS-PAGE gel and transferred onto a Trans-Blot nitrocellulose membrane (Whatman). The membrane was briefly rinsed in Tris-buffed saline containing 0.1% Tween 20 (TBS-T) and incubated for 1 h at room temperature in TBS-T containing 5% skim milk (Difco). The blocked membrane was incubated with the primary antibody (14-3-3, Santa Cruz Biotechnology, sc-629, 1:2000; CRM1, Santa Cruz Biotechnology, sc-5595, 1:500; Anti-GST, Millipore, 06-332, 1:1000) for 1 h at room temperature. Horseradish peroxidase-conjugated anti-rabbit or -mouse IgG (Zymed Laboratories Inc.) was used as the secondary antibody, and bound proteins were visualized with an ECL Western blotting detection system (GE Healthcare).

Intrinsic Tryptophan Fluorescence—We took advantage of the fact that α_2-S140(p) contains two tryptophan residues, which may show changes in either fluorescence intensity or wavelength with maximum emission following interaction of the peptide with another protein. Intrinsic tryptophan fluorescence spectra of the peptide alone or 14-3-3 alone (in 50 mM HEPES-KOH, pH 7.9, and 2 mM EDTA) were determined using a PerkinElmer Spectrofluorometer and served as controls. The excitation wavelength was set at 295 nm, and emission spectra were measured between 300 and 380 nm. Emission spectra were corrected by subtracting the spectrum of the peptide without excitation in the same buffer. The steady-state fluorescence spectrum of a sample containing 10 μM each of α_2-S140(p) peptide and 14-3-3 was then measured under the same conditions.

Isothermal Titration Calorimetry—ITC experiments were carried out using a VP-ITC microcalorimeter (MicroCal). His-tagged 14-3-3 proteins were dialyzed overnight into 50 mM HEPES (pH 7.9) containing 0.2 mM EDTA. From these samples, 25 μM solutions of monomeric subunits were placed in the cell chamber of the calorimeter (cell volume 1.4 ml). For most ITC

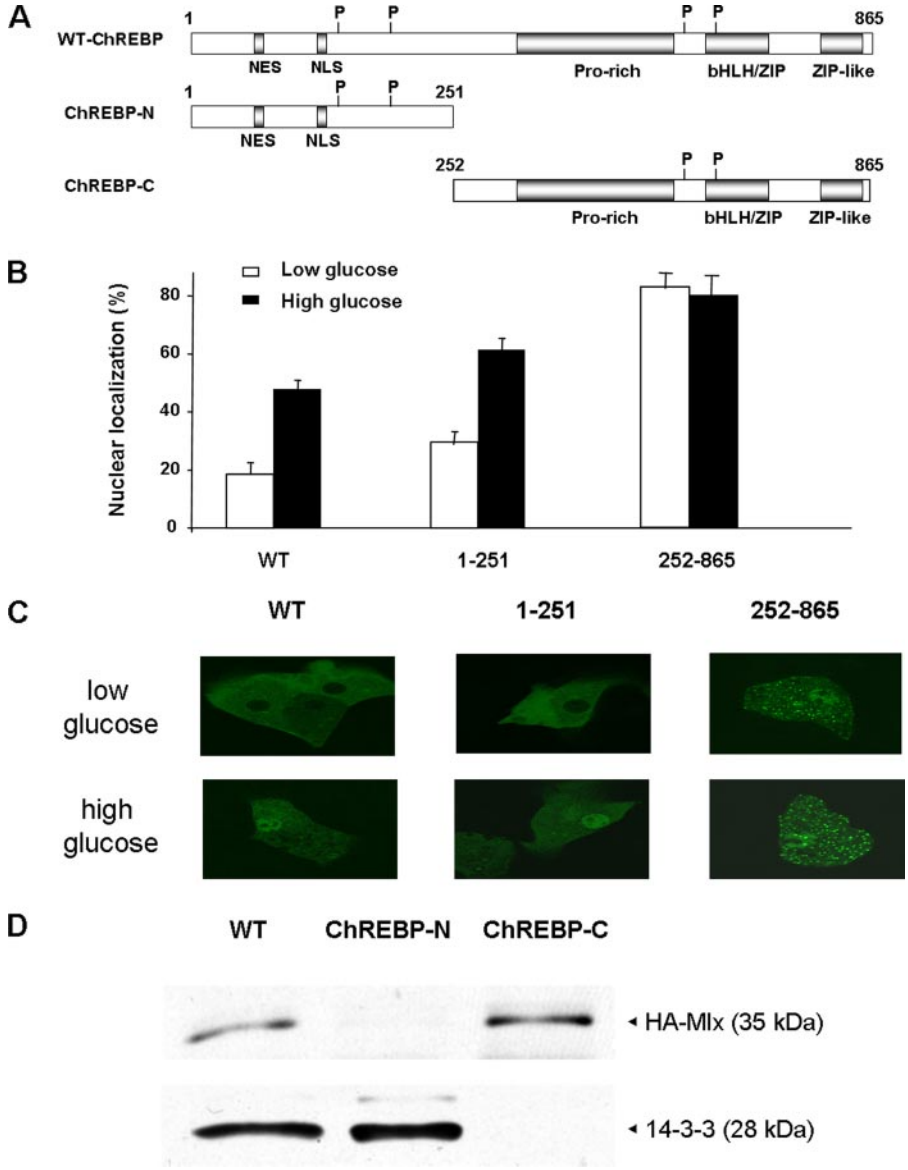

FIGURE 1. **The N-terminal region of ChREBP controls subcellular localization of ChREBP.** *A*, schematic depiction of the rat WT-ChREBP, ChREBP-N (residues 1–251), and ChREBP-C (residues 252–865) constructs of ChREBP. *B*, primary cultures of rat hepatocytes were transfected with GFP-tagged ChREBP proteins. The cells were cultured in DMEM containing 5.5 mM glucose, and then incubated for an additional 8 h with medium containing 5.5 (*open bars*) or 27.5 mM (*filled bars*) glucose. The cells were fixed with 4% formaldehyde, and subcellular localization of GFP-fused ChREBP was determined using confocal microscopy. The values presented are the mean ± S.D. of three sets of about 100 fluorescent cells. *C*, representative images showing subcellular localization of GFP-tagged WT-ChREBP, ChREBP-N, and ChREBP-C in rat hepatocytes. *D*, Mlx and 14-3-3 interactions with WT-ChREBP, ChREBP-N, and ChREBP-C. FLAG-tagged ChREBP proteins were immobilized on anti-FLAG beads, and incubated with HEK293T expressed HA-tagged Mlx or purified 14-3-3 for 1.5 h. The beads were collected, suspended in denaturing-SDS sample buffer, and analyzed by SDS-PAGE and immunoblotting using antibodies specific for HA tag or 14-3-3.

measurements either human or mouse 14-3-3β was used, but human 14-3-3 γ, ζ, and θ were also dialyzed and tested for binding to the phosphorylated ChREBP peptide α_2-S140(p). Readings were taken as α_2-S140(p) (or an unphosphorylated peptide, "α_2-Ser-140," prepared by treating α_2-S140(p) overnight with 1 microunit of calf thymus alkaline phosphatase) was added to the chamber from a syringe with an initial peptide concentration of 250 μM. All titration experiments were performed at 20 °C in 50 mM HEPES (pH 7.9) containing 0.2 mM EDTA. The ChREBP peptide was injected into the calorimetric cell in 12-μl increments. In all, 28 injections were made at 3-min intervals using a stirring speed of 310 rpm. As a reference, the ChREBP peptide was titrated into buffer, and the resulting readings were subtracted from the original 14-3-3 and ChREBP peptide titrations. The binding isotherm derived from heat changes was used to calculate the standard free energy of binding (ΔG°) according to the equation: $\Delta G^\circ = -RTInK_a$, where R is the gas constant, T the absolute temperature, and K_a the association constant. From the binding isotherm, the number of binding sites (n) was obtained, and changes in enthalpy (ΔH°) and entropy (ΔS°) were calculated according to the equation: $\Delta G^\circ = \Delta H^\circ - T\Delta S^\circ$. Curve fitting and the derivation of thermodynamic parameters were carried out with the ORIGIN version 7.0 software package (MicroCal). The concentrations of 14-3-3 proteins and the ChREBP peptide were determined using extinction coefficients at 280 nm of 25.7 and 13.98 $mM^{-1}\ cm^{-1}$, respectively.

Data Analysis—Statistical analysis was performed using GraphPad Prism5 software (GraphPad Software, San Diego, CA). Data were analyzed by one-way analysis of variance, followed by Newman-Keuls post hoc test, and groups designated with different letters are statistically different ($p < 0.05$).

RESULTS

The Distinct Roles of the N- and C-terminal Regions of ChREBP in Nuclear Localization and Transcriptional Activation—To better define the roles for the different domains of ChREBP, we expressed the N-terminal (residues 1–251; ChREBP-N) and C-terminal (residues 252–865; ChREBP-C) regions (Fig. 1*A*) of mouse ChREBP and determined their nuclear localization and transcriptional activation activity in primary rat hepatocytes. GFP-labeled ChREBP-N localized to the nucleus in the presence of high glucose but not low glucose, as determined by confocal microscopy (Fig. 1, *B* and *C*). This localization pattern was similar to that of wild type ChREBP (WT-ChREBP), but was distinct from the pattern we observed for ChREBP-C, which was distributed between the nucleus and cytosol under both glucose concentrations (Fig. 1, *B* and *C*). The approximately equal distribution of ChREBP-C in the nucleus and cytosol regardless of glucose

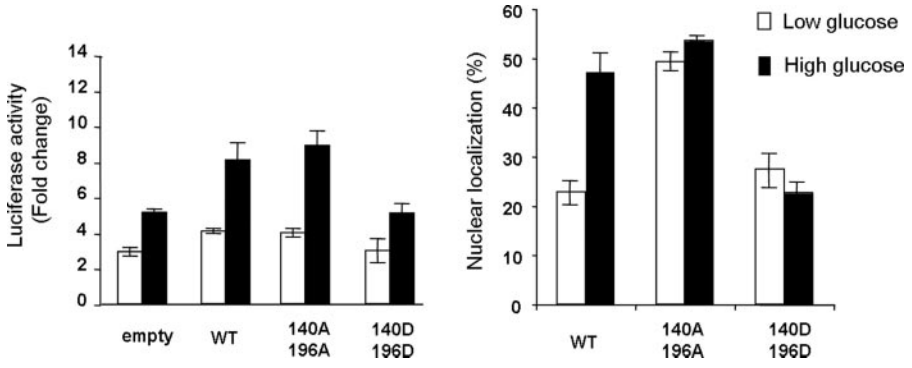

FIGURE 2. **Transcriptional activation and nuclear localization of wild type ChREBP and variants containing mutations at Ser-140 and Ser-196.** *Left*, primary cultured rat hepatocytes were co-transfected with pRL-TK (thymidine kinase promoter driving *Renilla* luciferase gene) as the internal control and pGL-3 Basic (expressing firefly luciferase under control of the rat LPK promoter region from −206 to −7). After transfection, cells were cultured in DMEM containing 5.5 mM glucose, and then incubated for an additional 12 h with medium containing 5.5 (*open bars*) or 27.5 mM (*filled bars*) glucose. Luciferase activity was measured and is expressed as firefly luciferase activity relative to *Renilla* luciferase activity. The values presented are the mean ± S.D. of replicate (three to four) cultures from a single experiment representative of more than three independent experiments. *Right*, nuclear localization of ChREBP in primary cultured hepatocytes. Primary cultured hepatocytes were transfected with GFP-tagged ChREBPs (wild type, S140A/S196A, and S140D/S196D). Cells were cultured in DMEM containing 5.5 mM glucose, and then incubated for an additional 8 h with medium containing 5.5 (*open bars*) or 27.5 mM (*filled bars*) glucose. The values presented are the mean ± S.D. of three sets of about 100 fluorescent cells.

levels suggests insensitivity of the C-terminal region to glucose concentration. These results clearly demonstrate that the N-terminal region, but not the C-terminal region, responds to glucose concentration and is fully responsible for nuclear localization of ChREBP in hepatocytes in the presence of high glucose levels.

ChREBP has been shown to interact with 14-3-3 (8) or Mlx (9, 20) to form heterodimers that function in subcellular localization and DNA binding, respectively. We tested the *in vitro* binding of these proteins to ChREBP by mixing them with FLAG-tagged ChREBP proteins immobilized on anti-FLAG beads, followed by centrifugation. ChREBP-N interacted exclusively with 14-3-3, consistent with its role in subcellular localization, whereas the ChREBP-C bound only Mlx, indicating its role in DNA binding (Fig. 1*D*). These results provided no evidence for a 14-3-3 binding site within the C-terminal region of ChREBP under these conditions, despite the previous suggestion of a site between residues 584 and 765 (8).

Regulation of ChREBP Activity by Phosphorylation of Ser-140 and Ser-196—Phosphorylation of residues Ser-140 and Ser-196 of ChREBP has been suggested to regulate nuclear translocation of ChREBP and its transcriptional activation status (4, 8), but the specific effects of phosphorylation are still controversial.

Here, we have focused on the effect of phosphorylation of Ser-140 and Ser-196 on nuclear localization and activation of transcription in hepatocytes. Using a transcription reporter assay, in which the ChREBP-activated LPK promoter drove the expression of the luciferase reporter enzyme (1), we found that WT-ChREBP and S140A/S196A-ChREBP were both activated 2.5-fold in high glucose (27.5 mM) relative to low glucose (5.5 mM) in hepatocytes (Fig. 2). In contrast, S140D/S196D-ChREBP, which mimics phosphorylation at both sites, had activity similar to the control (empty vector), which likely shows enhanced activity due to endogenous ChREBP in the hepatocytes. Similar results were obtained previously with the single S196D mutation, which mimics phosphorylation of only the Ser-196 site, relative to S196A-ChREBP (4).

Nuclear localization of GFP-tagged WT-ChREBP was 2-fold higher in high glucose conditions than in low glucose conditions in primary hepatocytes (Fig. 2). However, S140A/S196A-ChREBP localized to the nucleus in the presence of either high or low glucose, comparably to the levels we observed for WT-ChREBP in the presence of high glucose. This result indicates that mutation of these residues abolished glucose sensitivity. In contrast, the extent of nuclear localization of S140D/S196D-ChREBP at either glucose concentration was similar to that observed for WT-ChREBP in the presence of low glucose. A similar result was previously observed with S196D-ChREBP (4), although S140D/S196D-ChREBP was affected more significantly. These results suggest that phosphorylation of residues Ser-140 and Ser-196 inhibits nuclear localization of ChREBP under low glucose conditions. Moreover, mutation of these sites abolished the glucose sensitivity of nuclear localization but not of transcriptional activation, because the latter was still inhibited under low glucose conditions. One possible explanation for these results is that the N-terminal region of ChREBP is solely responsible for the glucose sensitivity of nuclear localization, whereas inhibition of transcriptional activation in low glucose may be chiefly mediated by phosphorylation of additional C-terminal sites such as Ser-626 or Thr-666 (4).

Taken together, these results suggest that the glucose sensitivity of nuclear localization of ChREBP is directly mediated by phosphorylation of residues Ser-140 and Ser-196. These phosphorylation sites are target sites for cAMP-dependent PKA or the related kinase PKG, consistent with the physiological observation that glucagon/cAMP signaling inactivates ChREBP in liver (21).

Interaction of ChREBP with a CRM1 Complex for Export—To determine the effect of phosphorylation of ChREBP on glucose-dependent changes in subcellular localization, we investigated the interactions of ChREBP with the proteins involved in cytoplasmic/nuclear trafficking. It is known that export of cargo proteins or RNAs from the nucleus requires the formation of a complex of the cargo with CRM1, Ran GTPase, GTP, and 14-3-3 (22). To test for formation of this complex *in vitro*, we mixed immobilized FLAG-WT-ChREBP (or the FLAG-ChREBP mutant proteins), with GTP and purified CRM1, 14-3-3, and a GTPase-dead variant of Ran (RanQ69L). ChREBP-bound proteins were eluted and subjected to SDS-PAGE and Western blotting with anti-14-3-3 and anti-FLAG antibodies. The 14-3-3 binding of the double D mutant increased much more than the additive effect of single D

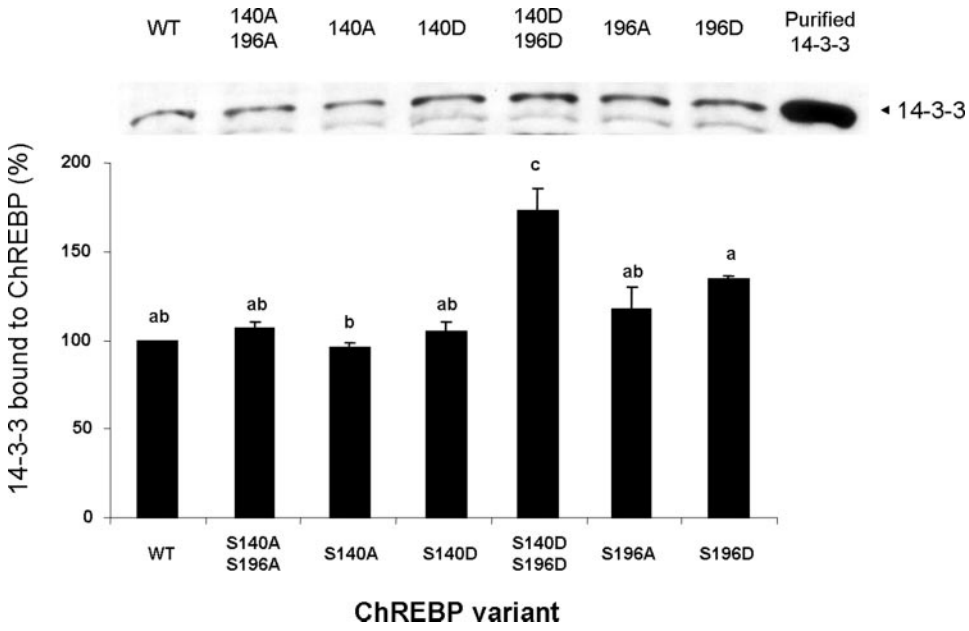

FIGURE 3. **14-3-3 binding to WT-ChREBP and various Ser-140/Ser-196-ChREBP alanine or aspartate mutants mimicking unphosphorylated and phosphorylated ChREBP, respectively.** FLAG-tagged ChREBP (wild type or bearing one or two mutations) were expressed in HEK293T cells, which were subsequently incubated for 48 h. FLAG-ChREBP in cell extracts was bound to anti-FLAG beads, which were then mixed with purified 14-3-3β in the presence of "export complex" including CRM1, Ran GTPase Q69L, and GTP. After 1 h the beads were washed and ChREBP-bound 14-3-3β was eluted and subjected to PAGE. Bound 14-3-3 proteins were measured by immunoblotting (*top*). The values presented are the mean ± S.D. of three sets of experiments (*bottom*). Significant differences among groups were determined by one-way analysis of variance followed by Newman-Keuls post hoc test. Groups designated with different letters are statistically different.

mutants, S140D/S196D ≫ S196D > S140D > WT, suggesting that there may be a cooperative effect of phosphorylation at the Ser-140 and Ser-196 sites (Fig. 3). In addition to this observation, the amino acid sequence around the phosphorylation site Ser-140 (RRKpSP) is related to the consensus 14-3-3-binding target (R*XXX*pSP, where *X* is any amino acid and pS is phosphoserine) (23).

Direct Interaction of ChREBP and Importin α for Nuclear Localization—Central to the nuclear transport process is a soluble import factor named importin β (or alternatively, karyopherin) (24–27). Importin β can bind cargo proteins either directly or indirectly through certain adaptor proteins, most commonly importin α. In pull-down assays (Fig. 4*A*), FLAG-tagged ChREBP interacted strongly with importin α but only weakly with importin β alone. However, importin β was readily incorporated into a complex with ChREBP and importin α (Fig. 4*A*), indicating that formation of the nuclear import complex between ChREBP and importin β is enhanced by importin α.

Effect of 14-3-3 on the Interaction of ChREBP with Importin α—Similar pull-down experiments were conducted to investigate whether ChREBP phosphorylation or the presence of 14-3-3 had any effect on the ChREBP/importin α interaction. In the presence of 14-3-3, the interaction of S140A/S196A-ChREBP with importin α was 2-fold greater than that of S140D/S196D-ChREBP or WT-ChREBP (Fig. 4*B*). This difference was less pronounced in the absence of 14-3-3. These results suggest that 14-3-3 masks the NLS of ChREBP (residues 158–173) and interferes with binding to importin α under conditions (such as low glucose) that favor export. Under high glucose conditions dephosphorylated ChREBP may bind to importin α more strongly, weakening the 14-3-3 interaction and thus exposing the NLS. This observation may be similar to a blockade by 14-3-3 of the NLS site of histone deactylase previously reported (27), but will require additional experiments to confirm. These results suggest that import and export of ChREBP are regulated in a reciprocal manner by the phosphorylation status of ChREBP, which directly affects the interactions of ChREBP with 14-3-3 and importin α.

Interaction of Highly Conserved α-Helices in the N-terminal Region of ChREBP with 14-3-3—Computational analyses of the secondary structure and helical propensity of ChREBP (14, 15) suggested the presence of three α-helices within the N-terminal 250 amino acids that are highly conserved among members of the related ChREBP and Mondo families of proteins. These helices consist of highly conserved residues at positions 85–95, 125–135, and 170–190 of ChREBP and are designated as α_1, α_2, and α_3, respectively (Fig. 5*A*). The α_1 helix is identical to the NES consensus sequence except for the presence of an extra Thr residue at the N-terminal end. The α_2 helix is within a region (residues 117–135) previously identified as a 14-3-3-binding site by Merla *et al.* (8). The N-terminal side of the α_3 helix overlaps with part of the NLS, and Ser-196, the PKA phosphorylation site, is just beyond its C terminus.

In hepatocytes, deletion of any of these α-helices eliminated the glucose-mediated nuclear localization of ChREBP (Fig. 5*B*) and transcriptional activation (Fig. 5*C*), indicating the importance of these helices (Fig. 5*B*). The α_1 deletion variant remained in the nucleus in the presence of either low or high glucose concentrations, which we attribute to the presence of the NES in this section. The result confirms that this site is likely involved in nuclear export of ChREBP. However, nuclear localization of the α_2 and α_3 deletion forms was inhibited 80 and 50%, respectively, and these ChREBP variants localized in the cytoplasm, resulting in loss of transcriptional activation activity (Fig. 5, *B* and *C*). These results suggest that the α_2 helix may be the primary 14-3-3 binding site of ChREBP and thus may be essential for export of ChREBP out of the nucleus.

Interaction of 14-3-3 with the α-Helix Deletion Variants of ChREBP—To study these conserved α-helices, we expressed FLAG-tagged ChREBP-N and three variant forms in which each of the α-helices described above was individually deleted. Coimmunoprecipitation of the 14-3-3 protein was abrogated when binding to the α_2 helix was deleted in the recombinant ChREBP protein (Fig. 6*A*). To determine whether the cytosolic localization of ChREBP was the result of interaction of the α-helices with 14-3-3, we expressed ChREBP-N and the α-helix

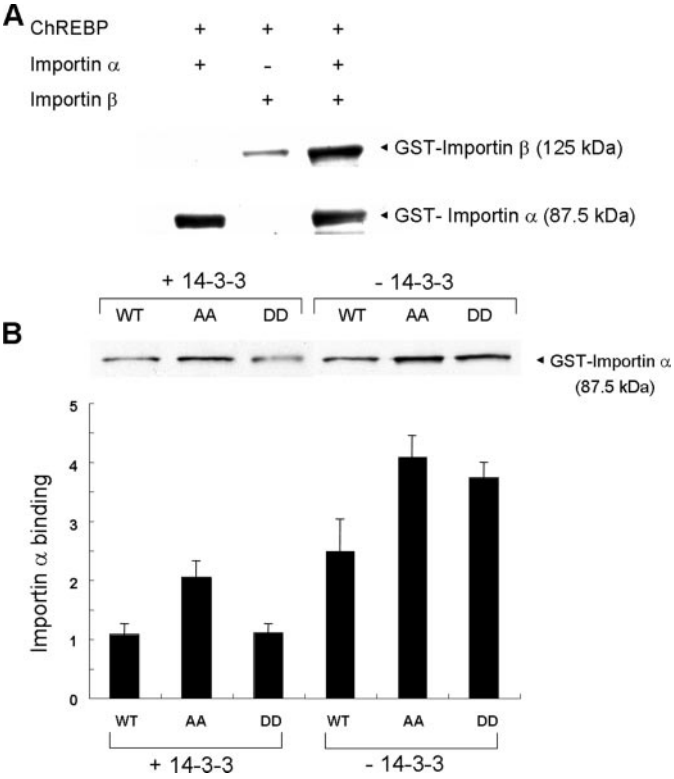

FIGURE 4. **Interaction of ChREBP with importin α, importin β, 14-3-3, and Mlx *in vitro*.** *A*, interaction of ChREBP with importin α and importin β. Co-immunoprecipitation assays were performed on purified GST-tagged importin α/β and lysates of HEK293T cells expressing FLAG-tagged ChREBP. ChREBP was pulled down by an anti-FLAG antibody and the pellets analyzed by Western blotting using an anti-GST antibody. These experiments were repeated three times. *B*, effect of 14-3-3 and mutations at Ser-140 and Ser-196 of ChREBP on the interaction of ChREBP with importin α. FLAG-tagged WT-ChREBP, S140A/S196A-ChREBP, or S140D/S196D-ChREBP were incubated with GST-tagged importin α in the presence and absence of 14-3-3. ChREBP was pulled down by an anti-FLAG antibody and analyzed by Western blotting using an anti-GST antibody. These reactions were carried out independently three times and a representative of these results is shown on the *top*. The *bar diagrams* were generated by scanning the immunoblots to quantitate the ChREBP binding to importin α in the presence and absence of 14-3-3β.

deletion mutants in HEK293T cells, which contain sufficient endogenous 14-3-3 to interact with the expressed forms of ChREBP, and incubated the cells under low glucose conditions. Nuclear and cytosolic fractions from these cells were passed through an anti-FLAG column, the bound proteins were eluted and subjected to SDS-PAGE, and ChREBP-N and the 14-3-3 proteins were identified by immunoblotting (Fig. 6*A*). Among the α-helix deletion variants of ChREBP-N, only the $\Delta\alpha_2$ variant failed to bind 14-3-3, indicating that the α_2 helix is the primary binding site, and the other helices may be less important for the interaction with 14-3-3. The α_2 helix of ChREBP is within a region (residues 117–135) previously suggested to be important for ChREBP protein-protein interactions (8).

Importance of α-Helical Structure for Interaction with 14-3-3—To evaluate the importance of the structure of the α_2 helix for binding 14-3-3, we prepared the following mutations within this motif of ChREBP: A129P and Y131P together, Y131P alone, and Y131K alone. Both Y131K and Y131P proteins weakly bound 14-3-3 compared with ChREBP-N, but A129P/Y131P-ChREBP-N, which we expect to lack this α-helix entirely, completely lost the ability to bind 14-3-3 (Fig. 6*B*). These results

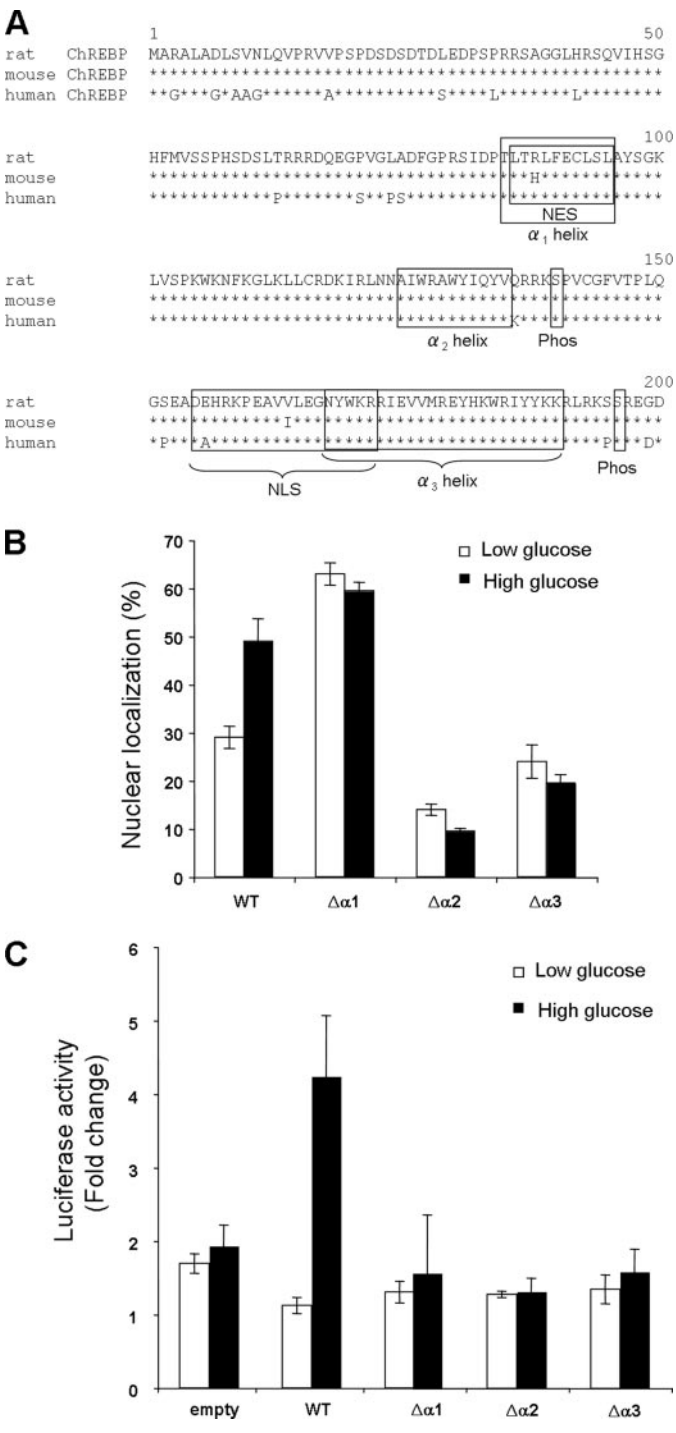

FIGURE 5. **Transcriptional activation and nuclear localization of ChREBP bearing α-helix deletion mutations.** *A*, residues 1–200 of ChREBP showing locations of the α_1, α_2, and α_3 helices, the NES, the NLS, and sites of phosphorylation. *B*, nuclear localization of GFP-tagged WT-ChREBP and the α_1, α_2, and α_3 deletion variants (Δα) of GFP-ChREBP. WT-ChREBP and the variant forms were expressed in HEK293T cells and incubated in the presence of low (*open bars*) or high (*filled bars*) glucose. Nuclear localization of the GFP-tagged proteins was determined using a confocal microscope. *C*, transcriptional activation activity of WT and α-helix deletion variants of ChREBP. DNA constructs expressing ChREBP proteins, firefly luciferase under control of the LPK promoter, and *Renilla* luciferase (an internal control) were cotransfected into primary cultured rat hepatocytes. Expressed luciferase activity was measured and is expressed as firefly luciferase activity relative to *Renilla* luciferase activity. The values presented are the mean ± S.D. of replicate (three or four) cultures from a single experiment representative of more than three independent experiments.

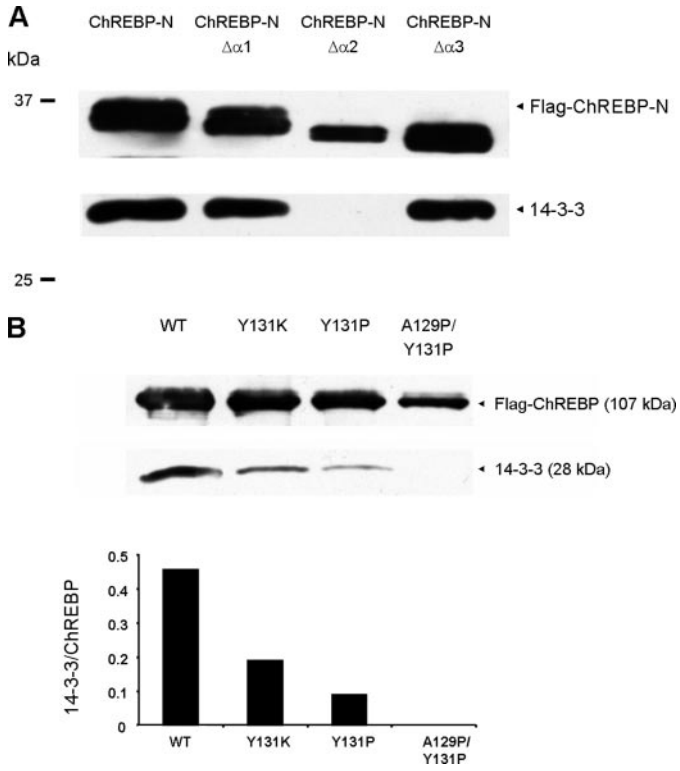

FIGURE 6. *A*, the α-helical structure of ChREBP is essential for its interaction with endogenous 14-3-3. HEK293T expressed FLAG-tagged ChREBP-N or ChREBP-N incorporating α-helix deletion mutations was incubated with endogenous 14-3-3 and the mixture was immunoprecipitated with anti-FLAG antibodies, subjected to SDS-PAGE, and Western blotted for immunodetection with antibodies against FLAG or 14-3-3. *B*, effect of mutation of the α_2 helix on the 14-3-3 binding. Co-immunoprecipitation assays of the cell lysates of HEK293T cells transfected with FLAG-tagged ChREBP variants (wild type, Y131K, Y131P, A129P/Y131P) and endogenous 14-3-3 were performed. ChREBP was pulled down using anti-FLAG antibody and the pellets were analyzed by SDS-PAGE and Western blotting as described in the legend to Fig. 6*A*.

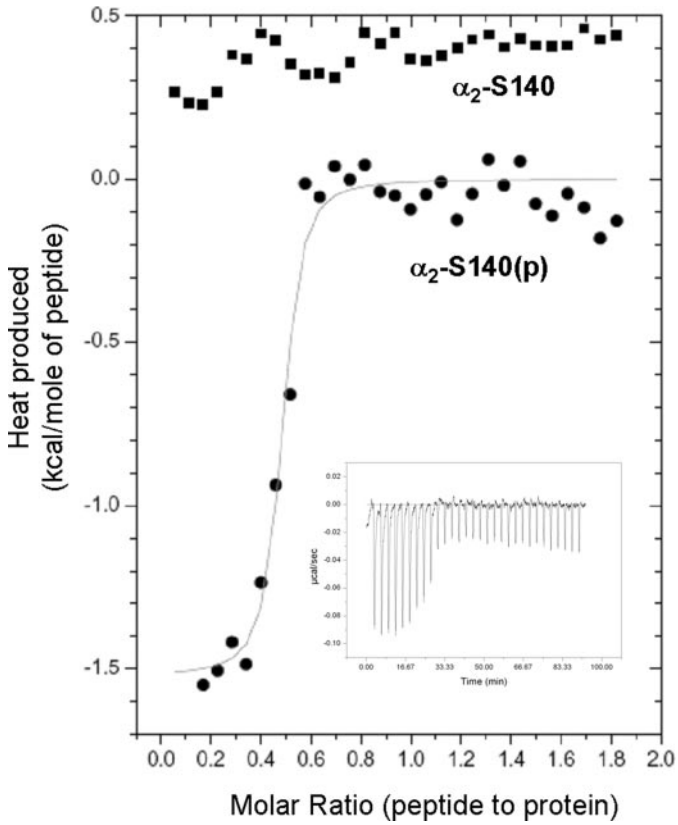

FIGURE 7. **Binding of human 14-3-3β and human ChREBP peptides measured by isothermal titration calorimetry.** Phosphorylated ChREBP peptide α_2-S140(p) (*closed circles*) or unphosphorylated ChREBP peptide α_2-S140 (*closed squares*) were titrated with human 14-3-3β. The *solid line* represents the line of best fit for the binding isotherm for α_2-S140(p) and human 14-3-3β, based on a single-site binding model using the ORIGIN version 7.0 software package. Data from the unphosphorylated ChREBP peptide α_2-S140 titrated with the 14-3-3 peptide were not fit with any binding models. The *inset* shows a thermogram for interaction of the 14-3-3β protein with α_2-S140(p). On *top*, the 14-3-3β binding to the unphosphorylated ChREBP peptide α_2-S140 is shown.

suggest that the α-helical structure of ChREBP is essential for interaction with 14-3-3.

Importance of Both the α_2 Helix and Phosphorylation of Ser-140 for 14-3-3 Binding—To obtain more direct physical evidence for the interaction between the α_2 helix and 14-3-3, we synthesized a peptide that included residues 125–142 of ChREBP. This sequence spans the α_2 helix and the Ser-140 phosphorylation site, and was designated α_2-S140(p). 14-3-3 proteins usually bind to one or two phosphorylated targets (23), but are also known to bind to unphosphorylated sites (28–31). Binding of 14-3-3β to the other phosphorylation site, Ser-196, was not investigated, because the distance between it and the α_2 helix is too large for a synthetic peptide.

We confirmed the α-helical nature of α_2-S140(p) in solution by circular dichroism (data not shown). We determined the thermodynamic parameters for the interaction of 14-3-3 with α_2-S140(p) using ITC. The heat generated by the interaction of human 14-3-3β with increasing concentrations of α_2-S140(p) allowed calculation of a K_d value of 0.45 μM and a stoichiometry (N) of 0.45 peptide molecules per 14-3-3 (Fig. 7). The dephosphorylated peptide after alkaline phosphatase treatment showed no detectable binding of 14-3-3 (*squares* in Fig. 7), demonstrating directly that phosphorylation of residue Ser-140 of the peptide is essential in addition to the α_2 helix for the interaction, and that they may act synergistically. Similar K_d and N values were obtained with mouse 14-3-3β (average K_d = 1.1 μM, n = 0.34).

α_2-S140(p) bound the other 14-3-3 isoforms, including 14-3-3γ, -ζ, and -θ, but with 30–50-fold lower affinities than the β isoform (Table 1), suggesting that the 14-3-3β binding sites for ChREBP may be different from those of the other 14-3-3 isoforms. One alternative is that the 14-3-3 binding sites for ChREBP occur at the same site, but possess lower affinities with different isoforms. The ITC measurements found the stoichiometry of ChREBP/14-3-3 binding to range between 0.34 and 0.54, suggesting that each dimer of 14-3-3 protein binds one peptide.

Because α_2-S140(p) contains two tryptophan residues (Trp-127 and Trp-130), we obtained additional evidence for the interaction between α_2-S140(p) and 14-3-3 by determining the effect of 14-3-3 on the fluorescence maxima and intensity of the peptide. The fluorescence emission spectrum of α_2-S140(p) was blue-shifted by 5 nm from 356 nm in the absence of 14-3-3 to 351 nm in its presence, without changes in fluorescence intensity (data not shown), suggesting a significant increase in the hydrophobicity around the tryptophan residues of α_2-S140(p) upon interaction with 14-3-3.

DISCUSSION

The subcellular localization of ChREBP in hepatocytes is controlled by its highly conserved N-terminal region. We propose in Fig. 8 the pathways that regulate the subcellular localization of ChREBP in response to glucose. Under low glucose conditions, ChREBP is phosphorylated at multiple sites and is mainly localized in the cytosol. In response to a rise in the circulating glucose concentration, Xu5P-activated PP2A dephosphorylates ChREBP, which then translocates into the nucleus (4, 5). Based on the data of the current studies we can now provide a more detailed itinerary for the cellular translocation of ChREBP in response to glucose (Fig. 8). ChREBP interacts with importin α, which allows complex formation with importin β and nuclear import. Inside the nucleus, any remaining phosphorylated residues are hydrolyzed by the same phosphatase, and ChREBP forms a complex with Mlx, resulting in DNA binding and transcription of target genes. Upon a drop in glucose concentration, ChREBP in the nucleus is phosphorylated to promote the formation of a complex with 14-3-3 and CRM1 for export out of the nucleus. The phosphorylated ChREBP may remain in a cytosolic complex with 14-3-3 and CRM1 until high glucose conditions reactivate it.

TABLE 1

Dissociation constants (K_d) for interactions of human or mouse 14-3-3 proteins with human ChREBP peptides as determined by isothermal titration calorimetry

Proteins	K_d
14-3-3β + α_2-S140(p)	1.1 μM
14-3-3β + α_2-S140	NM[a]
14-3-3γ + α_2-S140(p)	35 μM
14-3-3ζ + α_2-S140(p)	41 μM
14-3-3θ + α_2-S140(p)	>60 μM

[a] NM, not measurable.

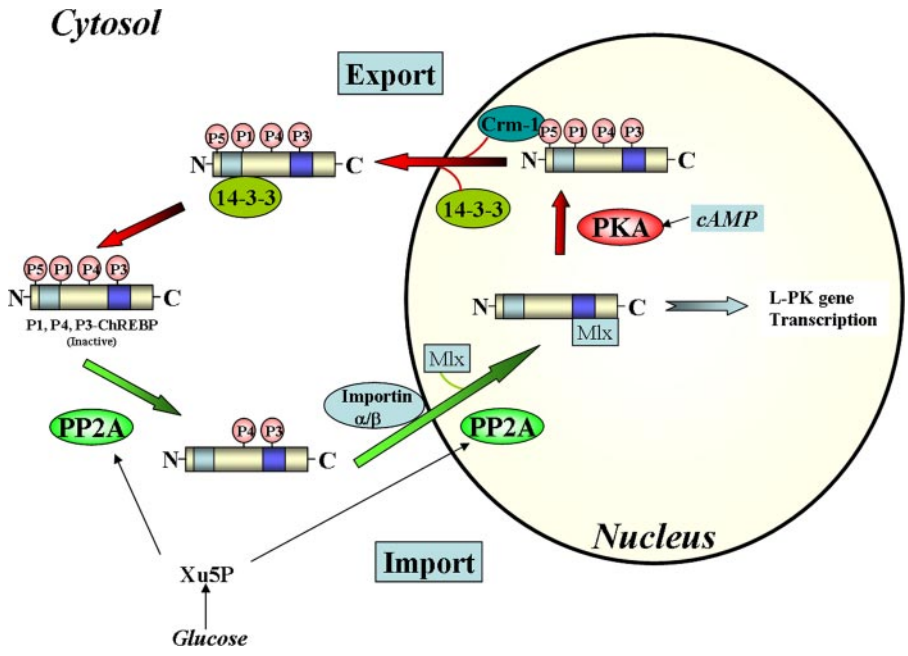

FIGURE 8. **Proposed nuclear-cytosol shuttle pathways of ChREBP.** In response to high glucose, phosphorylated, inactive ChREBP is dephosphorylated by Xu5P-activated PP2A, and translocates into the nucleus through interactions with importins α and β. There, ChREBP is further dephosphorylated by PP2A and induces transcription of LPK and lipogenic genes. A decrease in glucose concentration results in inactivation of ChREBP by phosphorylation by PKA and complex formation with 14-3-3 and CRM1 followed by translocation to the cytosol. The α_2-S140 indicates the titration with the substrate instead of the phosphorylated form.

One important finding of this work is that 14-3-3 binds to the α_2 helix of ChREBP and that this interaction is strengthened by neighboring phosphorylation site residues Ser-140 and Ser-196. We noted that the amino acid sequence adjacent to the phosphorylation site Ser-140 (RRKpSP) is the consensus 14-3-3-binding sequence (R*XXX*S(P)P, where *X* is any amino acid and Ser(P) is phosphoserine) (23).

Previously, Merla *et al.* (8) have shown using two-hybrid analysis that 14-3-3 proteins bind to the phosphorylated, but not the dephosphorylated, form of ChREBP through residues 117–134 of ChREBP as well as two other sites. They suggested that the phosphorylation-dependent interaction with 14-3-3 occurs indirectly or may be the result of conformational changes within ChREBP (8). The 117–134 peptide contains almost all of the predicted α_2 helix (residues 125–135) but lacks the Ser-140 phosphorylation site, which may explain its inability to bind 14-3-3. Our ITC measurements demonstrated that both the α_2 helix and phosphorylated Ser-140 are required for the 14-3-3/ChREBP interaction and that neither motif alone is sufficient.

In this study, we confirmed the observation that ChREBP interacts with the 14-3-3 proteins by means of a pull-down assay using FLAG-tagged full-length WT-ChREBP, the N-terminal region of ChREBP (residues 1–251), or full-length ChREBP variants containing mutations of Ser-140 and Ser-196, expressed in HEK293T cells. The interactions of these versions of ChREBP with 14-3-3 isoforms were confirmed by observing changes in tryptophan fluorescence and measuring production of heat when a short synthetic peptide containing the α_2 helix and S140(p) were mixed with 14-3-3. Based on these *in vitro* results we suggest that the 14-3-3 proteins bind to the α_2 helix and that the binding is regulated by the phosphorylation state of Ser-140 and possibly of Ser-196 as well. Indeed, phosphorylation of both of these sites resulted in significantly more binding than the singly phosphorylated forms.

It is unclear why others have failed to observe binding of 14-3-3 to S140D or S196D variants of ChREBP, even though ChREBP expressed in COS cells bound the 14-3-3 proteins (23, 32, 33) and alkaline phosphatase treatment abolished the binding (8). This cannot be due to differences between the phosphoryl residue and the aspartate side chain, because we observed that the biological activities of ChREBP bearing the same mutations, including nuclear localization and activation of transcription, were inhibited in hepatocytes and HEK293T cells (Figs. 2–4) (4). The different assay methods and types of cells used may have contributed to the differences in results. Other investigators have employed

the two-hybrid Gal4 method using ChREBP phosphorylated at various sites as bait (7, 8). In our study, we observed the protein-protein interactions using pull-down assays or biophysical measurements using short peptides; the results from these two techniques were entirely consistent. It is clear that methods focusing on a simple binding reaction between pure 14-3-3 proteins and a short synthetic ChREBP peptide appeared to produce greater effects than methods using full-length ChREBP. Moreover, different cell types exhibit significantly different glucose responses, which may also contribute to differences between our results and those of others. In our hands, primary hepatocytes are the only cell-type that responds appropriately to varying extracellular glucose concentrations.

The exciting new finding of this work is that ChREBP has a unique 14-3-3β binding site, different from other 14-3-3 target sites. The 14-3-3β binding site consists of the phosphorylation site(s) and an α-helix N-terminal to the Ser-140 (23, 32), whereas the other 14-3-3 isoforms bind only to the phosphorylation site(s). The binding affinity for the α_2-S140(p) peptide to 14-3-3β is 10-fold tighter than the α_2-S140(p) peptide than that observed for other 14-3-3 isoforms (Table 1). This increased binding affinity by 14-3-3β suggests that it may serve as the predominate partner for ChREBP in this cytosolic complex. This hypothesis is currently under investigation and will await future experiments.

Interestingly, opposing processes such as nuclear import and export are tightly regulated, often in a reciprocal manner. As shown in Fig. 8, low glucose conditions result in 14-3-3 binding to the NLS motif of ChREBP blocking importin α interactions resulting in inhibition of nuclear import. High glucose concentrations then lead to the following scenarios: 1) dephosphorylated ChREBP is dissociated from 14-3-3 leading to ChREBP binding to importin α for translocation into the nucleus and 2) 14-3-3 dissociation exposes the NLS site on ChREBP allowing ChREBP·importin α complex formation and nuclear import. In summary, we have shown that interaction of a specific helix of ChREBP with the 14-3-3 proteins plays an important role in the nuclear import and export of ChREBP, and that this interaction is regulated by phosphorylation of residues Ser-140 and Ser-196.

Acknowledgments—We thank Dr. Yoshihiro Yoneda, Osaka University Medical School, and Dr. Hisatoshi Shida, Hokkaido University, Hokkaido, Japan, for providing bacterial expression systems for importin α, importin β, and CRM1. We also thank Dr. Yuh Min Chook and Dr. Elliott Ross, Department of Pharmacology, University of Texas Southwestern Medical Center, for supplying Ran GTPase Q69L, and many valuable suggestions on fluorescence spectroscopy and the mechanism of action of the import/export factors.

REFERENCES

1. Yamashita, H., Takenoshita, M., Sakurai, M., Bruick, R. K., Henzel, W. J., Shillinglaw, W., Arnot, D., and Uyeda, K. (2001) *Proc. Natl. Acad. Sci. U. S. A.* **98,** 9116–9121
2. Nishimura, M., Fedorov, S., and Uyeda, K. (1994) *J. Biol. Chem.* **269,** 26100–26106
3. Kawaguchi, T., Osatomi, K., Yamashita, H., Kabashima, T., and Uyeda, K. (2002) *J. Biol. Chem.* **277,** 3829–3835
4. Kawaguchi, T., Takenoshita, M., Kabashima, T., and Uyeda, K. (2001) *Proc. Natl. Acad. Sci. U. S. A.* **98,** 13710–13715
5. Kabashima, T., Kawaguchi, T., Wadzinski, B. E., and Uyeda, K. (2003) *Proc. Natl. Acad. Sci. U. S. A.* **100,** 5107–5112
6. Tsatsos, N. G., and Towle, H. C. (2006) *Biochem. Biophys. Res. Commun.* **340,** 449–456
7. Li, M. V., Chang, B., Imamura, M., Poungvarin, N., and Chan, L. (2006) *Diabetes* **55,** 1179–1189
8. Merla, G., Howald, C., Antonarakis, S. E., and Reymond, A. (2004) *Hum. Mol. Genet.* **13,** 1505–1514
9. Cairo, S., Merla, G., Urbinati, F., Ballabio, A., and Reymond, A. (2001) *Hum. Mol. Genet.* **10,** 617–627
10. Ma, L., Tsatsos, N. G., and Towle, H. C. (2005) *J. Biol. Chem.* **280,** 12019–12027
11. Canbay, A., Bechmann, L., and Gerken, G. (2007) *Z. Gastroenterol.* **45,** 35–41
12. Stoeckman, A. K., Ma, L., and Towle, H. C. (2004) *J. Biol. Chem.* **279,** 15662–15669
13. Pozuelo Rubio, M., Geraghty, K. M., Wong, B. H., Wood, N. T., Campbell, D. G., Morrice, N., and Mackintosh, C. (2004) *Biochem. J.* **379,** 395–408
14. Cuff, J. A., Clamp, M. E., Siddiqui, A. S., Finlay, M., and Barton, G. J. (1998) *Bioinformatics* **14,** 892–893
15. Lacroix, E., Viguera, A. R., and Serrano, L. (1998) *J. Mol. Biol.* **284,** 173–191
16. Iizuka, K., Miller, B., and Uyeda, K. (2006) *Am. J. Physiol.* **291,** E358–E364
17. Hattori, M., Tugores, A., Veloz, L., Karin, M., and Brenner, D. A. (1990) *DNA Cell Biol.* **9,** 777–781
18. Nagoshi, E., Imamoto, N., Sato, R., and Yoneda, Y. (1999) *Mol. Biol. Cell* **10,** 2221–2233
19. Stewart, M., Kent, H. M., and McCoy, A. J. (1998) *J. Mol. Biol.* **284,** 1517–1527
20. Meroni, G., Cairo, S., Merla, G., Messali, S., Brent, R., Ballabio, A., and Reymond, A. (2000) *Oncogene* **19,** 3266–3277
21. Liu, Y. Q., and Uyeda, K. (1996) *Biochem. Biophys. Res. Commun.* **221,** 554–558
22. Pemberton, L. F., and Paschal, B. M. (2005) *Traffic* **6,** 187–198
23. Bridges, D., and Moorhead, G. B. (2004) *Sci. STKE* **2004,** re10
24. Cingolani, G., Petosa, C., Weis, K., and Muller, C. W. (1999) *Nature* **399,** 221–229
25. Gorlich, D., Henklein, P., Laskey, R. A., and Hartmann, E. (1996) *EMBO J.* **15,** 1810–1817
26. Mattaj, I. W., and Englmeier, L. (1998) *Annu. Rev. Biochem.* **67,** 265–306
27. Grozinger, C. M., and Schreiber, S. L. (2000) *Proc. Natl. Acad. Sci. U. S. A.* **97,** 7835–7840
28. Wang, B., Yang, H., Liu, Y. C., Jelinek, T., Zhang, L., Ruoslahti, E., and Fu, H. (1999) *Biochemistry* **38,** 12499–12504
29. Bodnar, R. J., Gu, M., Li, Z., Englund, G. D., and Du, X. (1999) *J. Biol. Chem.* **274,** 33474–33479
30. Masters, S. C., Pederson, K. J., Zhang, L., Barbieri, J. T., and Fu, H. (1999) *Biochemistry* **38,** 5216–5221
31. Seimiya, H., Sawada, H., Muramatsu, Y., Shimizu, M., Ohko, K., Yamane, K., and Tsuruo, T. (2000) *EMBO J.* **19,** 2652–2661
32. Yang, X., Lee, W. H., Sobott, F., Papagrigoriou, E., Robinson, C. V., Grossmann, J. G., Sundstrom, M., Doyle, D. A., and Elkins, J. M. (2006) *Proc. Natl. Acad. Sci. U. S. A.* **103,** 17237–17242
33. Liu, D., Bienkowska, J., Petosa, C., Collier, R. J., Fu, H., and Liddington, R. (1995) *Nature* **376,** 191–194